

Filter-feature-based rotation-invariant joint Fourier transform correlator

Farid Ahmed and Mohammad A. Karim

Rotation-invariant target detection using a trained filter-feature-based joint Fourier transform (JFT) correlator is investigated. First, a composite reference image is obtained from a training set of targets. An optimum filter formulation is then applied on this composite image to come up with a new feature that we refer to as a filter feature. This feature is then used in a JFT correlator, which results in a simple and robust rotation-invariant target recognition system. © 1995 Optical Society of America

1. Introduction

Classical matched correlation¹ and joint Fourier transform (JFT) correlation²⁻⁴ are the two most widely used techniques in optical pattern recognition. A phase-only filter⁵ and its variants were developed to improve correlation performance, however, none of these techniques is inherently rotation invariant. Rotation invariance in the literature is addressed in two different ways. The first approach uses geometric invariance properties in the filter formulation.⁶⁻⁸ For these studies circular harmonic filter expansion for rotation invariance was used. The main drawback with this method is that the performance depends on the choice of harmonic expansion center, which cannot be formulated in a systematic way. In the second approach, a number of rotationally shifted images are trained to design a filter, which is expected to respond favorably to all other rotated images. This is the synthetic discriminant filter (SDF) approach.^{9,10} A minimum-variance SDF¹¹ and a minimum-average correlation energy filter¹² are examples of two such composite filter formulations. The minimum-variance SDF has optimal noise tolerance, however, its application is limited by broader correlation peaks and sidelobes. On the other hand, the minimum-average correlation energy filter was designed to produce sharper correlation peaks to minimize average correlation plane energy, but it has poor noise tolerance. A limitation of both ap-

proaches is that they have suboptimal generalization capability, thus requiring a larger number of training patterns for an acceptable invariant recognition performance. On a related note, temporal multiplexing, which requires a mechanically rotating filter, has also been attempted for rotation-invariant detection.¹³ Use of filter modulation in SDF construction has already been proposed^{14,15} to improve invariance performance. A recent paper by Wang *et al.*,¹⁶ for example, reports some interesting results that pertain to such filter modulation. Modulation of the joint power spectrum (JPS) with a fringe-adjusted filter in a JFT correlator was also investigated¹⁷ to enhance the correlation discrimination. We propose herein a filter-feature-based composite filter formulation that is more optimal, flexible, and adaptive in nature. As far as implementation is concerned the JFT correlator is chosen, which generally uses a flexible setup. In this paper we first select training images with different in-plane rotations. The filter-feature descriptors of these training images are then determined. Among others, one of the goals here is to accentuate the high-frequency features of the images. It is a well-known fact that the dominance of low-frequency components contributes to broader correlation peaks.

2. Filter-Feature-Based Rotation-Invariant Joint Fourier Transform Model

The whole rotational distortion range is first divided into M different classes of distortion. This classification provides for a higher discrimination ratio and also results in an estimation of the degree of rotational distortion. For each class, a composite reference image is identified. Suppose that r_1, r_2, \dots, r_n are n rotationally distorted training images in class i . Let $s_i^1, s_i^2, \dots, s_i^n$ be the corresponding

The authors are with the Center for Electro-Optics, University of Dayton, 300 College Park Avenue, Dayton, Ohio 45469-0245.

Received 17 February 1995; revised manuscript received 30 May 1995.

0003-6935/95/327556-05\$06.00/0.

© 1995 Optical Society of America.

filter-feature training images obtained from the following transformation:

$$s_i^k = \mathcal{F}^{-1} \frac{D \exp(j\phi)}{|R_k| + a}, \quad (1)$$

where $|R_k| \exp(j\phi) = \mathcal{F}\{r_k\}$ and \mathcal{F} is the Fourier transform operator. The parameters a and D are, in general, functionally dependent on $|R_k|$. Since the operand $[D \exp(j\phi)/|R_k| + a]$ is Hermitian, s_i^k results in a real image. We investigate the effect of a for obtaining an optimal value that results in more invariant features through this transformation. Note that the above formulation, termed an amplitude-modulated phase-only filter, was first introduced to obtain better correlation discrimination.¹⁸ Here we use it as a feature extractor; hence the term filter feature.

One can compute and then synthesize all the features that employ Eq. (1) to construct the composite training feature c_i using the following relation:

$$c_i = s_i^1 + s_i^2 + \dots + s_i^n. \quad (2)$$

Therefore, in the input joint image of the JFT correlator we have M such composite features for M classes. These are then placed side by side in the reference half of the input joint image. With the input image t , the input joint image is then given by

$$g(x, y) = \sum_{i=1}^M c_i(x - x_i, y - y_i) + t(x, y), \quad (3)$$

where $c_i(x - x_i, y - y_i)$ represents the composite reference feature for class i , which is placed at the (x_i, y_i) location in the input joint image. The JFT of this input joint image results in

$$G(u, v) = \sum_{i=1}^M C_i(u, v) \exp(+jux_i + jvy_i) + T(u, v) \exp(-jv - ju). \quad (4)$$

The JPS is thus given by

$$\begin{aligned} |G(u, v)|^2 = & \sum |C_i(u, v)|^2 + |T(u, v)|^2 \\ & + \sum C_i(u, v) T^*(u, v) \exp(jux_i - jvy_i) \\ & + \sum C_i^*(u, v) T(u, v) \exp(-jux_i + jvy_i) \\ & + \sum_{l=1}^M \sum_{k=1, k \neq l}^M C_l(u, v) C_k^*(u, v) \\ & \times \exp[ju(x_l - x_k) + jv(y_l - y_k)]. \end{aligned} \quad (5)$$

The term $|C_i(u, v)|^2$, which is the magnitude squared Fourier transform of the synthesized composite feature c_i , is small compared with the other dc term $|T(u, v)|^2$. In reality, we can find a desired minimum value for this term with a proper choice of parameters D and a . This is a significant result in our approach, which further facilitates its JFT implementation.

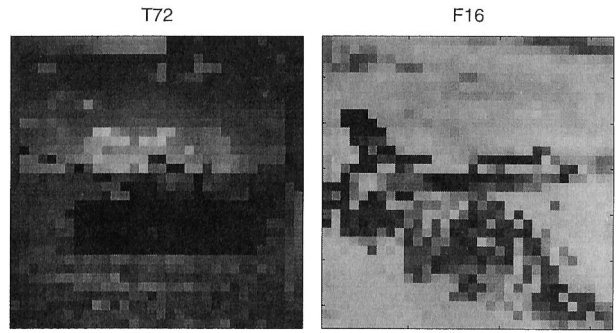


Fig. 1. Test images of the T72 tank (target) and the F16 aircraft (nontarget).

With the same above-mentioned reasoning, the last term of Eq. (5), which is the cross correlation among the synthesized composite features, does not contribute much to the JPS. Therefore, for all practical purposes, Eq. (5) can be approximated by

$$|G|^2 = |T|^2 + \sum_{i=1}^M (C_i T^* + T C_i^*). \quad (6)$$

Note again that elimination of the undesired dc and cross-correlation terms from the JPS is somewhat intrinsic in our filter-feature transformation. We found the output correlation by subtracting the zero-order term contributed by the input scene from the JPS and subsequently taking the inverse Fourier transform. Note that, in this approach, we get M output correlation peaks, each corresponding to one class of rotation.

3. Simulation Results

Let us consider $M = 3$ for a total distortion range of 0–90 deg. As far as the images are concerned, we use the T72 tank image (target) and the F16 aircraft (nontarget), as shown in Fig. 1. Each image is 32×32 in size, whereas the joint image of the joint transform correlator (JTC) is 256×256 . A block

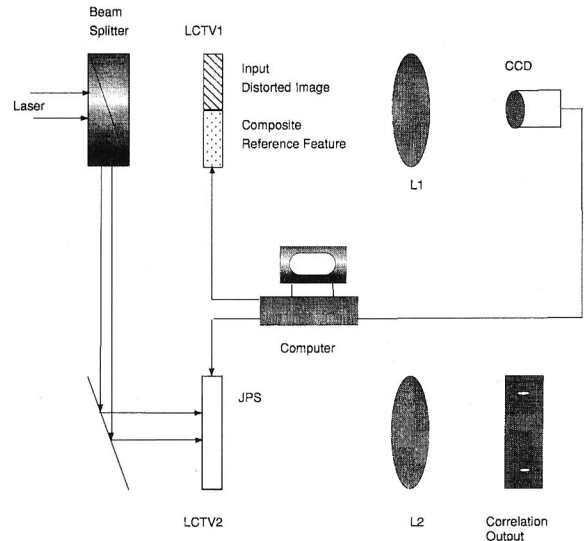


Fig. 2. Optical setup for the rotation-invariant JFT correlator.

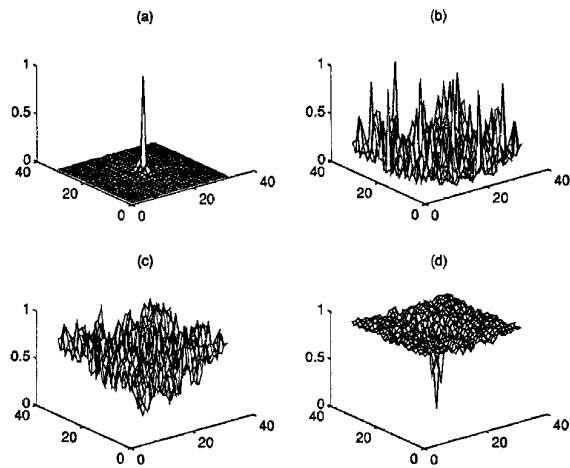


Fig. 3. (a) Fourier feature of the tank image; filter features of the tank image for (b) $\alpha = 0.1$, (c) $\alpha = 1$, and (d) $\alpha = 10$.

diagram representation for optical implementation of the proposed method is shown in Fig. 2. Note that the display of the JTC on a liquid-crystal television (LCTV) was originally proposed in Ref. 19. A light

source, such as a He-Ne laser, was used to illuminate the LCTV that displays the input distorted image and the composite reference features. The joint image is Fourier transformed by lens L1 and the intensity of the resulting image is detected by the CCD camera. The JFT image is then displayed on a second LCTV that can be illuminated by the same source using a beam splitter. The final inverse Fourier transform is performed by lens L2, and the correlation outputs are generated in the correlation plane.

First we selected the training images with different in-plane rotations. We consider an interval of 5 deg in the distortion range of 0–90 deg. This is then divided into $M = 3$ classes of distortion of 0–30, 30–60, and 60–90 deg. Therefore, in each class we have seven training images. The filter-feature descriptors of these training images are then determined. Figure 3 shows the Fourier feature and the proposed filter features [Figs. 3(b)–3(d)] of the target image (T72). The Fourier feature shown in Fig. 3(a) is only the Fourier transform of the image; one can obtain the filter feature using the formulation of Eq. (1). Note in particular how the high-frequency compo-

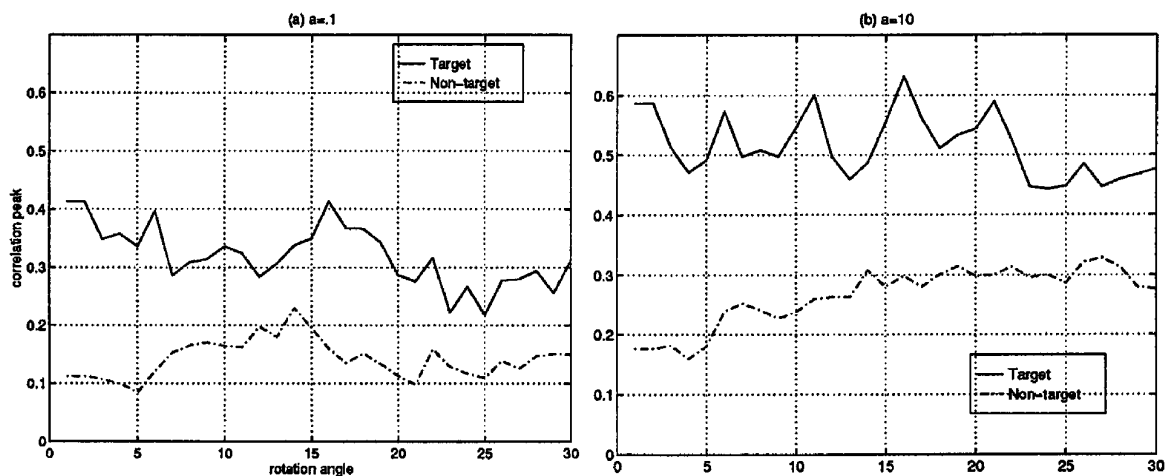


Fig. 4. Correlation performance in the 0–30-deg distortion range when (a) $\alpha = 0.1$ and (b) $\alpha = 10$.

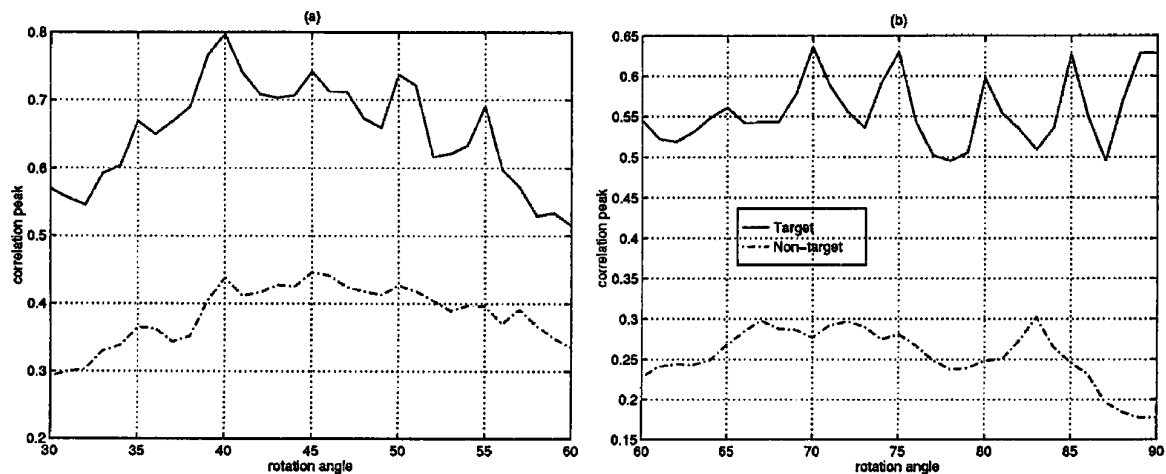


Fig. 5. Correlation performance in the distortion ranges of (a) 30–60 deg and (b) 60–90 deg.

Table 1. Discrimination Performance

Distortion Range (deg)	Discrimination Ratio
0–30	1.35
30–60	1.16
60–90	1.63

nents are enhanced by an increased value of parameter a when we use Eq. (1) as our new feature extractor. These new features are then synthesized to form the reference image of the JTC.

For testing the correlation performance we use distorted images at intervals of 1 deg. Figure 4 shows the correlation peak values from the JTC for different distorted images in the 0–30-deg range. It shows the discrimination between target and nontarget for two different values of parameter a . Within a certain range, the lower value for a results in a sharper correlation peak at the cost of a decrease in the correlation peak values and less discrimination, as seen from Figs. 4(a) and 4(b).

Figure 5 illustrates the corresponding correlation performance in the distortion ranges of 30–60 and 60–90 deg. For this and subsequent simulations we used a value of $a = 10$. Note that in each case we can set a threshold value for the correlation peak, above which the input can be treated as a target and below which it is a nontarget. To quantify the results further, we define the discrimination ratio (DR) as

$$DR = \frac{\text{minimum correlation peak}}{\text{maximum correlation peak}} \times \frac{\text{corresponding to target}}{\text{corresponding to nontarget}}. \quad (7)$$

Note that this worst-case DR is a conservative definition of the DR; an average DR is greater than this. Table 1 enumerates the DR values for different

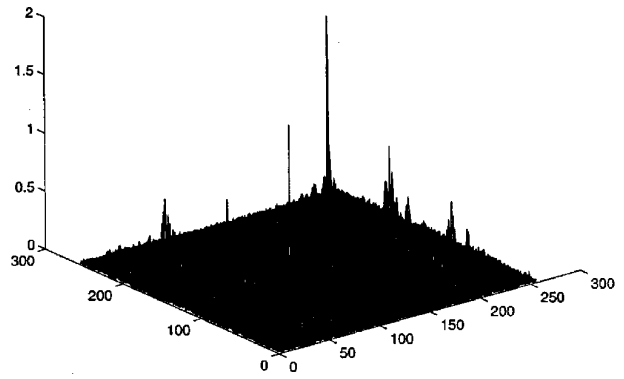


Fig. 7. Correlation output for a target rotated by 90 deg.

distortion ranges, which clearly shows that a threshold value can easily be set for the discrimination of a target from a nontarget for all possible ranges of rotational distortion of an input object.

Next, we place three composite reference images for the three classes of distortion into the input joint image. These are displaced to eliminate the effect of circular convolution. The input is now 91 distorted images of the target in the 0–90 range at intervals of 1 deg. We get three correlation peaks corresponding to the three classes of distortion. Figure 6(a) shows the results of this multireference JFT correlation. Note in particular how class 1 (0–30) performs well in the 0–30-deg distortion range, but its correlation performance is poor for the 30–90-deg range. In the

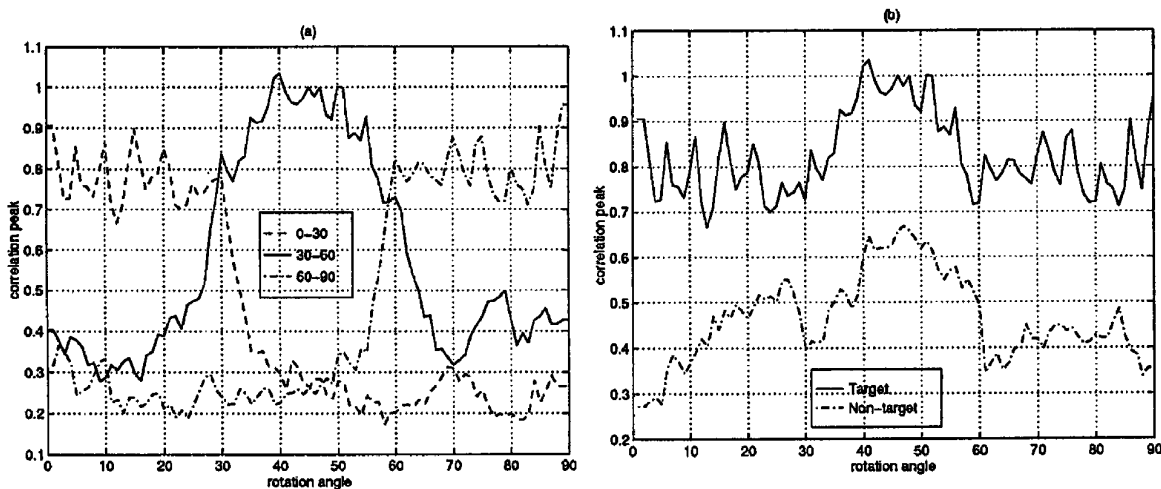


Fig. 6. (a) Correlation performance of the composite JTC for the target; (b) Correlation discrimination of the target and nontarget for the composite JTC.

shows the resulting discrimination between target and nontarget. Figure 7 shows the output correlation plot for a particular value of 90-deg distortion. Note that the peak corresponding to class 3 (60–90), which is in the upper right-hand corner of the correlation plane, is higher than the other two peaks. This indicates that the input distorted image is in class 3, in addition to the result that it can be isolated from a nontarget.

4. Conclusion

Rotation-invariant target detection based on filter feature of training images using a joint Fourier transform correlator has been presented. The feature transformation that we used for this study is highly optimal, flexible, and adaptive in nature. One appealing result is the composite reference feature formulation that uses only a simple superposition technique. When too many filters are superimposed, the use of such a technique can actually contribute to filter plane saturation. If the filters were orthogonal, saturation would become a nonissue. This scheme does not ensure orthogonalization of individual training filters; however, the number of training filters required herein is less compared with that required for a SDF. Accordingly, the problem of filter plane saturation is less critical in this technique. The SDF approach requires solving a constraint optimization problem. Our technique does not necessitate this computational complexity, yet it can be used to yield a promising rotation-invariant detection of targets.

References

1. A. VanderLugt, "Signal detection by complex spatial filtering," *IEEE Trans. Inf. Theory* **IT-10**, 139–145 (1964).
2. C. S. Weaver and J. W. Goodman, "A technique for optically convolving two functions," *Appl. Opt.* **5**, 1248–1249 (1966).
3. F. T. S. Yu and J. E. Ludman, "Microcomputer-based programmable optical correlator for automatic pattern recognition and identification," *Opt. Lett.* **11**, 395–397 (1986).
4. B. Javidi and C.-J. Kuo, "Joint transform image correlation using a binary spatial light modulator at the Fourier plane," *Appl. Opt.* **27**, 663–665 (1988).
5. J. L. Horner and P. D. Gianino, "Phase-only matched filtering," *Appl. Opt.* **23**, 812–816 (1984).
6. Y. N. Hsu and H. H. Arsenault, "Optical pattern recognition using circular harmonic expansion," *Appl. Opt.* **21**, 4016–4019 (1982).
7. F. T. S. Yu, X. Li, E. C. Tam, S. Jutamulia, and D. A. Gregory, "Rotation invariant pattern recognition with a programmable joint transform correlator," *Appl. Opt.* **28**, 4725–4727 (1989).
8. E. Elizur and A. A. Friesem, "Rotation-invariant correlation with incoherent light," *Appl. Opt.* **30**, 4175–4178 (1991).
9. C. F. Hester and D. Casasent, "Multivariant technique for multiclass pattern recognition," *Appl. Opt.* **19**, 1758–1761 (1980).
10. D. P. Casasent, "Unified synthetic discriminant function computational formulation," *Appl. Opt.* **23**, 1620–1627 (1984).
11. B. V. K. Vijaya Kumar, "Minimum-variance synthetic discriminant functions," *J. Opt. Soc. Am. A* **3**, 1579–1584 (1986).
12. A. Mahalanobis, B. V. K. Vijaya Kumar, and D. Casasent, "Minimum average correlation energy filters," *Appl. Opt.* **26**, 3633–3640 (1987).
13. S. Jutamulia and T. Asakura, "Rotation-invariant joint transform correlator," *Appl. Opt.* **33**, 5440–5442 (1994).
14. D. A. Jared and D. J. Ennis, "Inclusion of filter modulation in synthetic-discriminant-function construction," *Appl. Opt.* **28**, 232–239 (1989).
15. M. B. Reid, P. W. Ma, J. D. Downie, and E. Ochoa, "Experimental verification of modified synthetic discriminant function filters for rotation invariance," *Appl. Opt.* **29**, 1209–1214 (1990).
16. R. K. Wang, C. R. Chatwin, and M. Y. Huang, "Modified filter synthetic discriminant functions for improved optical correlator performance," *Appl. Opt.* **33**, 7647–7654 (1994).
17. M. S. Alam and M. A. Karim, "Fringe-adjusted joint transform correlation," *Appl. Opt.* **32**, 4344–4350 (1993).
18. A. A. S. Awwal, M. A. Karim, and S. R. Jahan, "Improved correlation discrimination using an amplitude-modulated phase-only filter," *Appl. Opt.* **29**, 233–236 (1990).
19. F. T. S. Yu, S. Jutamulia, T. W. Lin, and D. A. Gregory, "Adaptive real-time pattern recognition using a liquid crystal TV based joint transform correlator," *Appl. Opt.* **26**, 1370–1372 (1987).